4028 J. Med. Chem. 2010, 53, 4028–4037
DOI: 10.1021/jm100023j

Journal of Medicinal Chemistry Article

Discovery of *N*-[(4*R*)-6-(4-Chlorophenyl)-7-(2,4-dichlorophenyl)-2,2-dimethyl-3,4-dihydro-2*H*-pyrano[2,3-*b*]pyridin-4-yl]-5-methyl-1*H*-pyrazole-3-carboxamide (MK-5596) as a Novel Cannabinoid-1 Receptor (CB1R) Inverse Agonist for the Treatment of Obesity

Lin Yan,*[,†] Pei Huo,[†] John S. Debenham,[†] Christina B. Madsen-Duggan,[†] Julie Lao,[‡] Richard Z. Chen,[‡] Jing Chen Xiao,[‡] Chun-Pyn Shen,[‡] D. Sloan Stribling,[§] Lauren P. Shearman,[§] Alison M. Strack,[§] Nancy Tsou,[⊥] Richard G. Ball,[⊥] Junying Wang,[∥] Xinchun Tong,[∥] Thomas J. Bateman,[∥] Vijay B. G. Reddy,[∥] Tung M. Fong,[‡,#] and Jeffrey J. Hale[†]

Departments of [†]Medicinal Chemistry, [‡]Metabolic Disorders, [§]Pharmacology, [∥]Drug Metabolism and Pharmacokinetics, and [⊥]Pharmaceutical Research and Development, Merck Research Laboratories, P.O. Box 2000, Rahway, New Jersey 07065.
[#] Current address: Forest Research Institute, Jersey City, New Jersey 07311.

Received January 8, 2010

This paper describes the discovery of *N*-[(4*R*)-6-(4-chlorophenyl)-7-(2,4-dichlorophenyl)-2,2-dimethyl-3,4-dihydro-2*H*-pyrano[2,3-*b*]pyridin-4-yl]-5-methyl-1*H*-pyrazole-3-carboxamide (MK-5596, **12c**) as a novel cannabinoid-1 receptor (CB1R) inverse agonist for the treatment of obesity. Structure−activity relationship (SAR) studies of lead compound **3**, which had off-target hERG (human ether-a-go-go related gene) inhibition activity, led to the identification of several compounds that not only had attenuated hERG inhibition activity but also were subject to glucuronidation in vitro providing the potential for multiple metabolic clearance pathways. Among them, pyrazole **12c** was found to be a highly selective CB1R inverse agonist that reduced body weight and food intake in a DIO (diet-induced obese) rat model through a CB1R-mediated mechanism. Although **12c** was a substrate of P-glycoprotein (P-gp) transporter, its high in vivo efficacy in rodents, good pharmacokinetic properties in preclinical species, good safety margins, and its potential for a balanced metabolism profile in man allowed for the further evaluation of this compound in the clinic.

Introduction

Obesity is a global epidemic.[1] A World Health Organization (WHO[a]) 2006 survey of the United States found that 67% of adults aged 20 and above are overweight ($25 \leq \text{BMI} < 30$) or obese ($\text{BMI} \geq 30$). Globally, obesity is alarmingly on the rise, particularly in developing countries. There are approximately 400 million obese people aged 15 and above and over 1.6 billion overweight in 2005. Obesity is a major risk factor for a number of chronic diseases, including diabetes, cardiovascular diseases, and some forms of cancer. The treatment cost of obesity- and overweight-related illnesses has placed a substantial burden on health care resources: In 2008 the United States alone spent $147 billion.[2]

The fundamental cause of obesity is the excess consumption versus expenditure of calories. Advances in science and technology have made energy-dense food readily available and led to lifestyles requiring less physical activity. While obesity can be potentially treated via a low calorie diet, physical exercise, and a balanced lifestyle, the mechanism of energy homeostasis can make it difficult for overweight and obese people to lose weight by voluntarily eating less.[3] Although regulation of energy homeostasis is complex and many aspects of it are still unknown, the endocannabinoid system, particularly cannabinoid-1 receptor (CB1R), has been indicated to play an important role in regulating energy balance.[4]

Cannabinoid-1 receptor is a G-protein-coupled receptor widely expressed in the central nervous system (CNS) and also in peripheral tissues. Both preclinical and clinical studies have demonstrated that blocking CB1R activity with antagonists or inverse agonists can reduce body weight and food intake.[5] Consequently, the development of CB1 antagonists and inverse agonists as therapeutic agents has been the subject of intense research in the pharmaceutical industry. Merck Research Laboratories have previously disclosed several CB1R inverse agonists.[6] A novel acyclic CB1R inverse agonist, taranabant (MK-0364, **1**), was evaluated in clinical trials as a potential treatment for obesity (Figure 1).[7] Compound **1** is a potent CB1R inverse agonist and reduces body weight and food intake in both human and rodents through CB1R-based mechanism. Compound **1** is primarily metabolized by CYP3A4 enzyme and therefore has the potential to be affected by CYP3A4 inhibitors. The objective for the backup program is to develop a CB1R inverse agonist that has CB1R pharmacological

*To whom correspondence should be addressed. Phone: (732) 594-5419. Fax: (732) 594-2200. E-mail: lin_yan@merck.com.

[a]Abbreviations: WHO, World Health Organization; BMI, body mass index; CB1R, cannabinoid-1 receptor; CB2R, cannabinoid-2 receptor; CNS, central nervous system; DIO, diet-induced obese; GABA, γ-aminobutyric acid; SAR, structure−activity relationship; hERG, human ether-a-go-go related gene; PyBOP, benzotriazol-1-oxytripyrrolidinophosphonium hexafluorophosphate; ee, enantiomeric excess; CHO, Chinese hamster ovary; CP-55,940, (1*R*,3*R*,4*R*)-3-[2-hydroxy-4-(1,1-dimethylheptyl)-phenyl]-4-(3-hydroxypropyl)cyclohexan-1-ol; cAMP, cyclic adenosine monophosphate; MK499, *N*-[1′-(6-cyano-1,2,3,4-tetrahydro-2*R*-naphthalenyl)-3,4-dihydro-4*R*-hydroxyspiro(2*H*-1-benzopyran-2,4′-piperidin)-6-yl]-methanesulfonamide; HEK, human embryonic kidney; d-Fen, dexfenfluramine; MED, minimal efficacious dose; P-gp, P-glycoprotein efflux transporter.

 Published on Web 04/27/2010

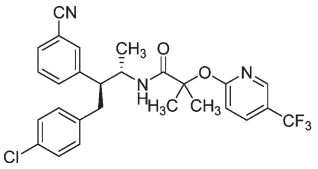

1 MK-0364 (Taranbant)
$CB1R\ IC_{50}$ 0.3 nM
$CB2R\ IC_{50}$ 290 nM

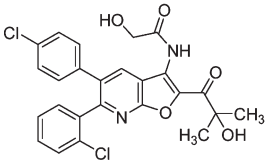

2 Furanopyridine lead
$CB1R\ IC_{50}$ 4.3 nM
$CB2R\ IC_{50}$ 5400nM

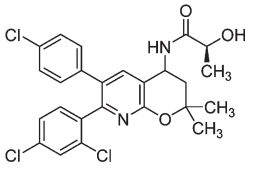

3 Pyranopyridine lead
$CB1R\ IC_{50}$ 4.8 nM
$CB2R\ IC_{50}$ 2260 nM

Figure 1. Merck early leads of CB1R inverse agonists.

profile similar to **1** but is less dependent on CYP3A4 for clearance.[8]

Recently, two new series of CB1R inverse agonists bearing fused pyridine bicyclic cores were discovered by Merck scientists.[9] Furanopyridine **2** is a potent CB1R inverse agonist and induced overnight body weight loss and food intake suppression in DIO rats (MED $\approx$ 0.3 mg/kg); however, it caused mild to pronounced hyperactivity, hyperreactivity, and ataxia at doses of 30−100 mg/kg in conscious mice, possibly because of its partial agonism of $\alpha1\beta3\gamma2$ $GABA_A$ receptor subtype. SAR studies of **2** led to the identification of several fused bicyclic pyridine series of CB1R inverse agonists. Among them, pyranopyridine **3** was a potent CB1R inverse agonist and efficacious in DIO rats. Although devoid of $GABA_A$ off-target activity, compound **3** had potent off-target inhibition of hERG potassium channel. In this paper, we will describe the SAR studies of **3** that lead to the discovery of a potent and efficacious CB1R inverse agonist **12c** (MK-5596)[10] with attenuated off-target hERG activity. This compound has a CB1R activity profile similar to that of **1** but with a more balanced metabolic profile.

Chemistry

Pyranopyridine compounds discussed in this paper were prepared according to two general methods: a racemic synthetic route (Scheme 1)[9b] and an asymmetric synthetic method (Scheme 2). At the earlier stage of SAR studies, pyranopyridines were prepared according to the racemic synthetic method. Treatment of 5-(4-chlorophenyl)-6-(2,4-dichlorophenyl)-2-oxo-1,2-dihydropyridine-3-carbonitrile with 2-methyl-1-propenylmagnesium bromide followed by acidic hydrolysis gave ketone **5** (Scheme 1). Condensation of **5** with hydroxylamine provided oxime **6**, which was subsequently reduced by zinc dust in acetic acid to amine **7**. A variety of acids were coupled to **7** using PyBOP as the coupling reagent, and the resulting mixture of amides **8** were then separated by chiral chromatography to give two enantiomers or four diastereomers, if a chiral acid was used. For clarity, only the more active enantiomer or diastereomers will be discussed in this paper. To expedite the SAR study, an asymmetric synthesis of the penultimate amine was developed using Noyori's asymmetric hydrogen transfer reaction (Scheme 2).[11] By use of ruthenium catalyst, i.e., Ru-(1*S*,2*S*)TsDPEN prepared from $[RuCl_2(\eta^6\text{-arene})]_2$

Scheme 1[a]

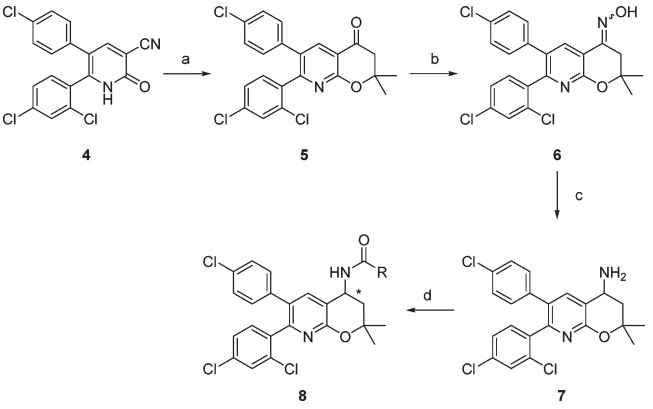

[a] (a) (1) 2-methylpropenylmagnesium bromide, THF, 50 °C, 16 h; (2) pH $\sim$ 3, room temp, 5 h (78% over two steps); (b) $H_2NOH\cdot HCl$, NaOAc, Et_3N, THF, CH_3OH, 70 °C, 16 h; (c) Zn, HOAc, 95 °C, 2 h (70% over two steps); (d) (1) RCO_2H, PyBOP, Et_3N, CH_2Cl_2, room temp (70−100%); (2) chiral HPLC separation.

Scheme 2[a]

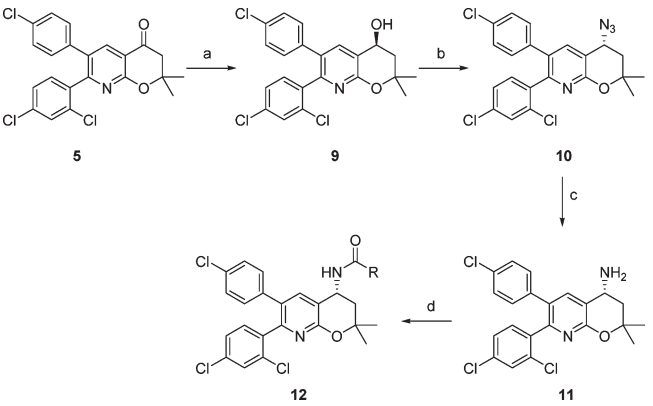

[a] (a) Ru-(1*S*,2*S*)TsDPEN, IPA, CH_2Cl_2 room temp, 16 h (69%); (b) $Zn(N_3)_2(pyridine)_2$, PPh_3, imidazole, DIAD, CH_2Cl_2, room temp (92%); (c) $P(CH_3)_3$, H_2O, THF, room temp (80%); (d) RCO_2H, PyBOP, Et_3N, CH_2Cl_2, room temp (76% to quant).

and (1*S*,2*S*)-*N*-(*p*-toluenesulfonyl)-1,2-diphenylethylenediamine, ketone **5** was reduced to *S*-alcohol **9** in >99% ee.[12] *S*-Alcohol **9** was then stereospecifically converted to *R*-azide **10**, which was subsequently reduced to amine **11** in >98% ee.[13,14] Similarly, a variety of acids were readily coupled to amine **11** using PyBOP.

Results and Discussion

Synthesizing compounds that are cleared by multiple metabolic enzymes could minimize the potential for drug−drug interactions in humans.[15] Phase II metabolism may occur directly on the parent compounds that contain appropriate functional groups. It is therefore conceivable that by incorporation of such functional groups, drug clearance will be less dependent upon phase I metabolism, which is often mediated by cytochrome P450 enzymes, for clearance, making them less susceptible to CYP450 mediated drug−drug interactions. Previous studies have shown that the hydroxyl group of glycolic amide in **2** undergoes rapid glucuronidation (one class of phase II metabolism) in dog; however, no formation of glucuronide conjugate of **3** was detected. It was thus hypothesized that the appropriate amide group in an analogue

of **3** might lead to the identification of functional groups that undergo direct glucuronidation across species as well as minimize off-target hERG activity.

The CB1R and CB2R binding affinities (IC_{50}) of test compounds were determined in competitive binding assays with membranes of Chinese hamster ovary (CHO) cells stably expressing recombinant human CB1R and CB2R using [^{3}H]CP-55,940 as ligand.[16] The CB1R and CB2R functional potencies (EC_{50}) as inverse agonists were measured by inhibition of forskolin-stimulated intracellular cAMP increase of CB1R and CB2R expressing CHO cells. All compounds discussed in this paper were found to be CB1R inverse agonists. Off-target hERG inhibition of test compounds was measured by competitive inhibition of [^{35}S]MK499 binding to hERG channel expressed in HEK-293 cell membranes.[17] The relative propensity of test compounds to undergo phase II metabolism was tested by the detection of metabolites following incubation with rat and human hepatocytes.[18] Compounds exhibiting direct conjugation (i.e., glucuronidation) as a major metabolic pathway were predicted to be less vulnerable to CYP mediated drug−drug interactions. Active compounds, especially those without off-target activities and/or capable of glucuronidation, were tested in an acute pharmacodynamic model (usually at a dose of 3 mg/kg) for pharmacological efficacy to evoke overnight body weight loss and food intake suppression in DIO rats.

During the initial phase of SAR studies, compounds were prepared using a racemic synthesis followed by chiral HPLC separation. Comparison of the values of CB1R inhibition (IC_{50}) of these enantiomers generally showed at least greater than 5-fold difference. In order to expedite the SAR study, an asymmetric synthesis was developed. Table 1 compares the CB1R binding affinities and hERG inhibition activities of two exemplary pairs of enantiomers. Compound **13**, an *R*-enantiomer, was a potent CB1R inverse agonist with 3 orders of magnitude selectivity over CB2R, while its corresponding *S*-enantiomer **14** was about 50 times less potent as CB1R inhibitor. The discrepancy of CB1R binding affinities was much greater between compounds **15** and **16**. Although compound **15** showed effectively no detectable hERG binding at the highest testing concentration (30 μM), no formation of a glucuronide conjugate of **15** was detected. These comparisons established that the higher CB1R binding activity of pyranopyridine series was largely associated with the *R*-configuration.

A series of compounds containing functional groups with the potential for glucuronidation were designed and synthesized. Their biological activities were compared with those of the lead compound **3** in CB1R/CB2R selectivity, off-target hERG activity, potential of glucuronidation, and acute overnight body weight loss and food intake suppression in DIO rats (Table 2). Lead compound **3** was a potent CB1R inverse agonist with greater than 1000-fold selectivity against CB2R and had good pharmacokinetics in rat ($t_{1/2}$ = 7.9 h and F = 100%). Oral administration of **3** at doses of 1 and 3 mg/kg to DIO rats resulted in body weight loss of −6 and −16 g and food intake suppression of −28% and −72% vs vehicle treated animals (+5 g weight gain and 0%), respectively. Compound **3**, however, was a potent hERG inhibitor (IC_{50} = 120 nM), and its hydroxyl group did not form a glucuronide conjugate following incubation with both rat and human hepatocytes. Increasing the lipophilicity around the lactamide of **3** by introducing a methyl group led to compound **8a**, which had in vitro and in vivo CB1R activity

Table 1. Effects of Compound's Chirality on Binding Affinities of CB1R and CB2R and Inhibition of hERG Potassium Channel Are Exemplified by Two Pairs of Pyranopyridine Enantiomers[d]

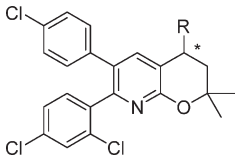

No.	Stereochemistry	R	CB1/CB2 IC_{50} (nM)[a]	hERG IC_{50} (μM)[b]
13	*R*	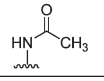	1.2/1200	0.54
14	*S*		56/9400	2.66
15	*R*	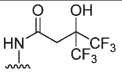	1.1/56	>30
16	*S*	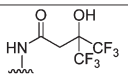	480/17000	ND[c]

[a] Competitive CB1R and CB2R binding against CP-55,950. Data are reported as the mean for n = 2 measurements. SD is generally within ±20% of the average. [b] Competitive hERG binding against MK499. Data are reported as the mean for n = 2 measurements (n = 1 when IC_{50} > 30 μM). SD is generally within ±20% of the average. [c] Not determined. [d] The chiral center is marked by an asterisk (*).

profiles similar to **3** but did not form a glucuronide conjugate. Formation of a glucuronide conjugate of the parent was detected following incubation with both human and rat hepatocytes for compound **8b**, which had a cyclopropane group replacing the geminal dimethyl group of **8a**; however, **8b** was still a potent hERG inhibitor (IC_{50} = 300 nM). Replacement of the lactamide methyl group of **3** with a trifluoromethyl group provided compound **8c** that was capable of forming a glucuronide conjugate of the parent following incubation with both rat and human hepatocytes. The strong electron-withdrawing effect of trifluoromethyl group was expected to increase the acidity of the hydroxyl group and thus might enhance its potential for undergoing glucuronidation.

Compound **8c** was a potent CB1R inverse agonist with good selectivity against CB2R and exhibited robust overnight food intake suppression and body weight loss in DIO rats at a dose of 1 mg/kg. However, it still inhibited hERG channel at low concentration. The other active diastereomer **8d** also showed similar potent hERG inhibition. Increasing steric hindrance around the hydroxyl group of **8d** by introducing a methyl group led to **8e** that did not improve its selectivity against hERG inhibition, although it remained as a potent CB1R inverse agonist. By movement of the trifluoroethanol group one carbon away from the amide carbonyl of **8c** and **8e**, compound **8f** was a 10-fold less potent hERG inhibitor than **3** while still forming a glucuronide conjugate of the parent. Compound **8f** was about 4 times more potent as CB1R inverse agonist than **3**, but it showed less significant in vivo efficacy at a dose of 3 mg/kg, although it had good pharmacokinetics in rat ($t_{1/2}$ = 8.2 h and F = 41%). The other active diastereomer **8g** was also less active in acute DIO rat study. Finally, the hydroxyl group of 2,2-difluoro-3-hydroxypropanamide in **8h** also allowed for glucuronidation, but it was still a potent

Table 2. Comparison of CB1R and CB2R Binding Activities, Off-Target hERG Binding Activities, Potential for Glucuronidation, and Effects of Test Compounds on the Acute Overnight Body Weight Change (ΔBW) and Food Intake (FI) Suppression vs Vehicle (veh.) in Diet-Induced Obese (DIO) Rats[i]

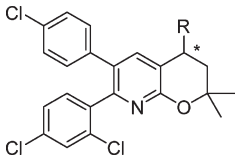

No.	R	CB1/CB2 IC_{50} (nM)[a]	hERG IC_{50} (μM)[b]	Glucur. Human/Rat[c]	Overnight BW and FI Change[d]		
					Dose (mg/kg)	ΔBW (g)[e] (veh.)	% ΔFI[e] vs. veh.
3		3.0/4800	0.12	No/No	3	-16 (+5)	-72
					1	-6 (+5)	-28
8a		1.7/2500	0.38	No/No	3	-11 (+5)	-48
8b[f]	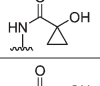	6.5/3000	0.30	Trace/Trace	3	-14 (+7)	-74
8c	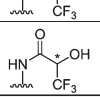	1.8/3400	0.26	Yes/Yes	1	-5 (+5)	-28
8d	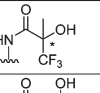	0.3/1400	0.41	ND[g]	ND	ND	ND
8e	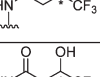	0.7/1400	0.60	Trace/Trace	3[h]	-4 (+6)	-27
8f	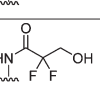	0.7/250	1.46	Trace/Trace[h]	3	+2 (+5) $p = 0.16$	-1 $p = 0.96$
8g	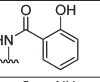	1.7/220	2.47	Trace/Trace[h]	1	+4 (+9) $p = 0.12$	-6 $p = 0.58$
8h	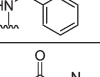	0.6/1300	0.08	Trace/Trace	ND	ND	ND
12a	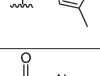	4.0/3300	>30	Yes/Yes	3	+1 (+8) $p = 0.08$	-25
12b	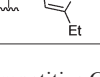	1.3/350	>30	Trace/Trace	3	+1 (+6)	-1 $p = 0.88$
12c	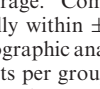	1.0/1500	1.0	Yes/Trace	3	-13 (+6)	-57
					1	-7 (+8)	-35
12d	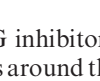	2.1/500	1.2	Trace/Yes	3	-7 (+10)	-48

No.	R	CB1/CB2 IC_{50} (nM)[a]	hERG IC_{50} (μM)[b]	Glucur. Human/Rat[c]	Overnight BW and FI Change[d]		
					Dose (mg/kg)	ΔBW (g)[e] (veh.)	% ΔFI[e] vs. veh.
12e	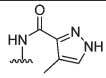	0.2/2200	5.3	Trace/No	3	-9 (+5)	-40
					1	+1 (+5)	-26
12f	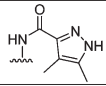	0.5/1400	8.7	Trace/No	3	0 (+10)	-26
12g	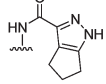	1.4/530	>30	Trace/Trace	3	-6 (+6)	-13 $p = 0.13$
12h	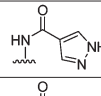	0.2/3400	0.38	No/No	3	+2 (+5) $p = 0.16$	-3 $p = 0.80$
12i	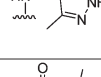	0.3/1400	1.1	Trace/No	3	-8 (+5)	-36
					1	+2 (+7)	-17
12j	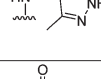	0.2/2300	1.6	Yes/No	3	-10 (+5)	-58
					1	0 (+7)	-34
12k	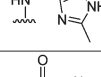	2.0/5200	2.0	ND	1	+2 (+10)	-21
12l	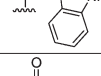	0.6/14000	4.6	No/Trace	3	+2 (+8) $p = 0.07$	-25 $p = 0.16$
12 m	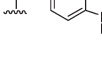	0.6/2700	0.63	No/No	ND	ND	ND
12n	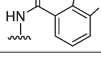	1.3/1900	>30	No/No	1	+3 (+5) $p = 0.31$	-3 $p = 0.63$

[a] Competitive CB1R and CB2R binding against CP-55,950. Data are reported as the mean for $n \geq 2$ measurements. SD is generally within ±20% of the average. [b] Competitive hERG binding against MK499. Data are reported as the mean for $n = 2$ measurements ($n = 1$ when $IC_{50} > 30\,\mu M$). SD is generally within ±20% of the aveage. [c] Glucuronidation of parent compound. Trace describes glucuronidation levels that are detectable by mass spectrographic analysis but do not represent a significant metabolic pathway. [d] Overnight body weight gain and food intake suppression in DIO rat (n = 6−8 rats per group). [e] All $p < 0.05$ unless otherwise noted. [f] Only racemic mixture was tested. [g] Not determined. [h] Experiments were performed on racemic mixtures. [i] The chiral center is marked by an asterisk (*).

hERG inhibitor. By modulation of the steric and electronic effects around the lactamide of **3**, most of the compounds were still potent CB1R inverse agoinsts. Several compounds were found to form glucuronide conjugates of the parent and also attenuate off-target hERG activity; however, none of them showed in vivo activities comparable to **3** in the acute pharmacodymanic model.

Next we examined the replacement of the lactamide of **3** with aryl groups containing functional groups for glucuronidation. Phenol of compound **12a**, as expected, formed a glucuronide conjugate by both human and rat hepatocytes, but it only exhibited low in vivo activity, probably due to its poor bioavailability in rat ($t_{1/2}$ = 1.9 h and F = 1%). Formation of a glucuronide conjugate of the anilinic amine group in **12b** was also detected. Like **12a**, compound **12b** did not induce significant in vivo biology activity because of its low bioavailability in rat ($t_{1/2}$ = 7.4 h and F = 5%). Replacing phenyl group with pyrazole

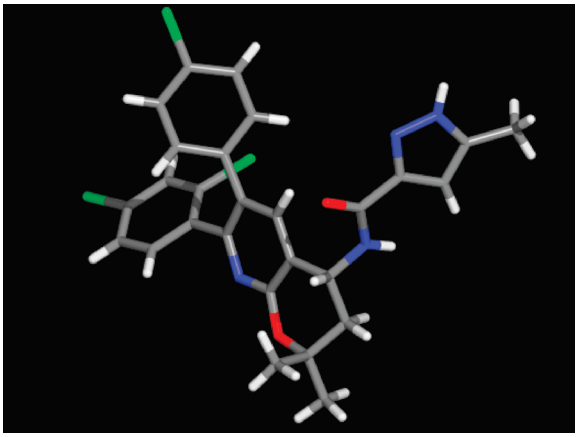

Figure 2. X-ray crystallography analysis confirmed the absolute stereochemistry of compound **12c** as *R*.

resulted in compound **12c**, which is a potent CB1R inverse agonist, and reduced food intake and body weight at a dose of 3 mg/kg in DIO rats. In addition, compound **12c** was a weak hERG inhibitor (IC_{50} = 1 μM) and formation of a glucuronide conjugate of the parent was detected following incubation with both human and rat hepatocytes. By extension of methyl at C4 to ethyl, **12d** was slightly less active than **12c** in the acute PD model. Transposing the methyl group from C4 to C5 gave **12e**, which was 5-fold more potent and 5-fold more selective against hERG than **12c**, suggesting substitution at C5 might enhance selectivity against hERG. Formation of a glucuronide conjugate of **12e** was detected, and in vivo efficacy in DIO rats was similar to that of **12c** at a dose of 3 mg/kg. Compounds **12f** and **12g** with substitution on C5 were more selective against hERG but less efficacious in lowering body weight and suppressing food intake in DIO rats than **3**. Interestingly, no formation of a glucuronide conjugate of the pyrazole **12h** was detected, while **12i** and **12j** with substitutions on the pyrazole ring generated glucuronide conjugates of parent. Both compounds were potent CB1R inverse agonists and had similar efficacy as that of **12c** at a dose of 3 mg/kg. Conversion of **12c** into triazole **12k** did not result in compounds with good pharmacodynamic efficacy. Finally, formation of glucuronide conjugates of indazole **12l** was detected in the presence of rat hepatocytes, while no glucuronide conjugate formation for indazole **12m**, and **12n** was detected. Although **12l** was a potent CB1R inverse agonist, it did not induce body weight loss and food intake suppression comparable to **12c**.

It was possible to differentiate among these four new active compounds (**12c**, **12d**, **12h**, and **12i**) based on their ability to drive a pharmacodynamic response, i.e., reduction of body weight and food intake, at lower dose (1 mg/kg). Compound **12c** emerged as the most potent compound to cause overnight body weight loss and food intake suppression at a dose of 1 mg/kg. It has greater than 1000-fold of selectivity of CB1R over CB2R in both human and rat (rCB1R and rCB2R IC_{50} of 0.7 and 1500 nM, respectively) and is an inverse agonist (EC_{50} = 5.8 nM, −111% inverse agonism) of human CB1R. The absolute structure of **12c** was confirmed to be *R* by X-ray crystallographic analysis (Figure 2). Its corresponding *S*-enantiomer was prepared and found to be less potent as a CB1R inverse agonist (IC_{50} = 7.65 nM) and more potent as a hERG inhibitor (MK499 IC_{50} = 0.67 μM) than **12c**. On the

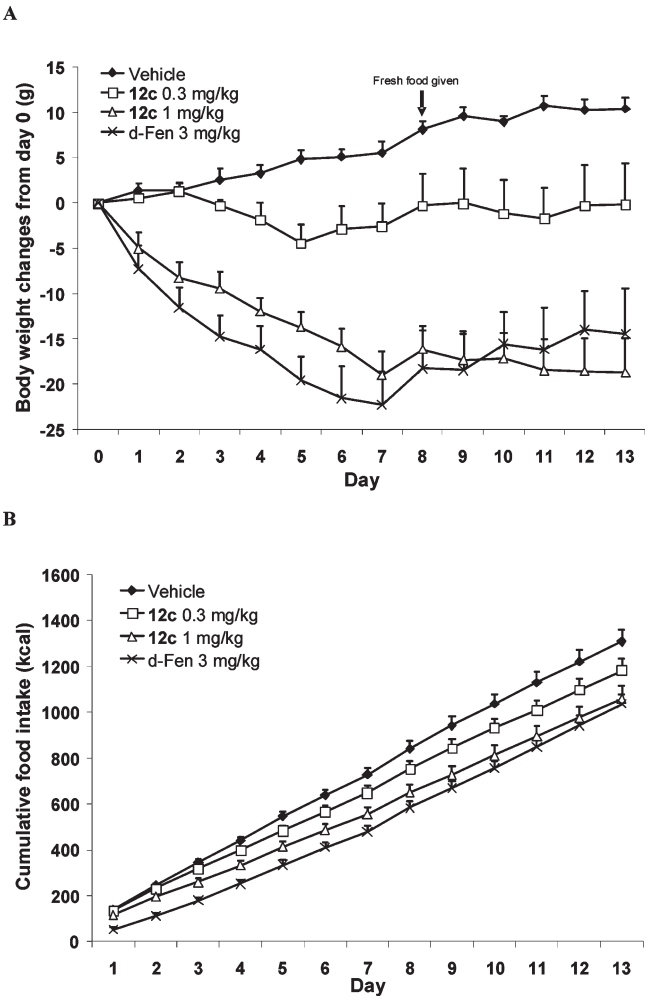

Figure 3. Chronic efficacy studies of compound **12c** dosed at 0.3 and 1 mg/kg in DIO rats: (A) daily body weight change; (B) cumulative food intake. Fresh food was given on day 8. Last measurement was conducted 18 h after dosing of test compound on day 13. In all graphs, data represent the mean ± SEM (n = 7−8 rats per group).

basis of its potent CB1R binding affinity, attenuated inhibition of off-target hERG potassium channel, acute pharmacodynamic efficacy, and potential for phase II metabolism in human, compound **12c** was chosen for further pharmacokinetic and pharmacodynamic characterization and metabolism profiling in preclinical species.

Chronic efficacy of compound **12c** was evaluated by comparing body weight loss and food intake suppression of **12c**-treated group of DIO rats to those of vehicle- and d-Fen-treated groups over a period of 13 days. Compound **12c** produced a dose-dependent lowering of body weight (Figure 3A). Average body weight gain of the vehicle-treated group over 13 days was 10 ± 1 g. Cumulative body weight changes from starting weight in the 0.3 and 1 mg/kg groups were −0 ± 5 and −19 ± 4 g, respectively. The final relative body weight loss compared with vehicle was 1.6% and 4.5% for the 0.3 and 1 mg/kg groups, respectively. As a positive control, the 3 mg/kg d-Fen-treated group produced an incremental body weight loss up to day 7 and then gradually body weight loss decreased. In comparison, **12c** at a dosage of 1 mg/kg generated a sustained body weight loss up to day 13 with the final body weight loss comparable to that of the 3 mg/kg d-Fen group. Compound **12c** also generated a dose-dependent

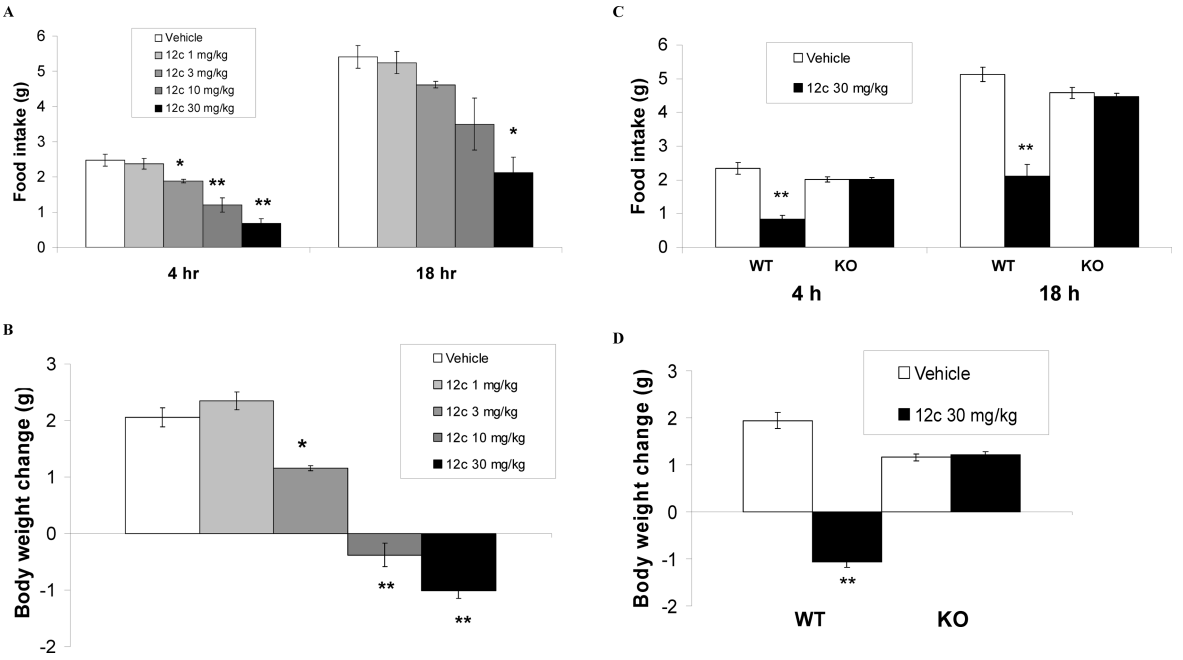

Figure 4. Comparison of effects of **12c** on food intake and body weight gain between lean wide type (WT) mice and CB1R knockout (KO) C57BL/6 mice. Effects of compound **12c** on ad libitum food intake of WT C57BL/6 mice (A) and overnight body weight gain in WT mice (B). Ad libitum fed lean mice (6−7 months of age, BW ≈ 29 g) were dosed orally ~30 min prior to dark phase. Diet was switched from regular chow to medium high fat diet (D12266) upon dosing. Mice were weighed 4 and 18 h (overnight) after dosing. Mean and SEM are shown (n = 6−7 per group): (*) $P < 0.05$ or (**) $P < 0.01$ vs vehicle (one-way ANOVA and Dunnett's test for multiple comparison). Effects of **12c** (30 mg/kg) on food intake of WT mice (6−7 months of age, BW ≈ 28 g) or KO mice (6−7 months of age, BW ≈ 25 g) (C) and overnight body weight gain of WT or KO mice (D). Mean and SEM are shown (n = 10 per group): (**) $P < 0.01$ vs corresponding vehicle (unpaired t test).

food intake suppression in DIO rats (Figure 3B). In comparison with the vehicle-treated group, the reductions in cumulative food intake of **12c**-treated group were 10 ± 4% and 19 ± 4% for the 0.3 and 1 mg/kg groups, respectively. The 1 mg/kg **12c**-treated group exhibited cumulative food intake suppression similar to that of the 3 mg/kg d-Fen-treated group. The minimal efficacious dose (MED) of the 13-day chronic study was determined to be 0.3 mg/kg. At the end of the chronic efficacy study, the levels of compound **12c** (18 h after the last dose, 0.3 mg/kg) were determined to be 180 ± 40 nM in plasma and 110 ± 30 nM in brain, respectively, and the corresponding ratio of brain and plasma exposure was calculated to be 0.63. For comparison, a 13-day parallel pharmacokinetics study was carried out in DIO rats and the exposures of compound **12c** (24 h after the last dose, 0.3 mg/kg) were determined to be 135 ± 59 nM in plasma and 74 ± 15 nM in brain, respectively, and thus the brain and plasma ratio was 0.55. This chronic study demonstrated that compound **12c** had good brain penetration and required low plasma exposure to drive in vivo efficacy to reduce body weight and food intake in DIO rats.

The antiobesity effect of **12c** was examined in CB1R knockout mice.[19] In ad libitum fed wild-type lean mice (C57BL/6), compound **12c** caused a dose-dependent reduction in food intake (Figure 4A) and a reduced overnight body weight gain or even a reduction in body weight (Figure 4B). The MED for **12c** in lean mice was determined to be 3 mg/kg. In contrast, compound **12c** did not show significant effects on food intake (Figure 4C) or body weight (Figure 4D) at a dose of 30 mg/kg in CB1R knockout mice. The lack of in vivo efficacy in CB1R-deficient mice suggested that the anorectic effects observed for **12c** were due to a CB1R-mediated mechanism.

Incubation of **12c** in both human and rat liver microsomes produced predominately oxidative metabolite M2 (data not shown). In the presence of anti-CYP3A4 antibodies, incubation of **12c** did not yield M2 in human liver microsomes, indicating that the oxidative metabolism of this compound was CYP3A4 dependent. Additional studies were conducted in both rat and human hepatocytes to observe both phase I and phase II metabolism of **12c**. Following incubation with rat hepatocytes the predominant metabolic route of **12c** was oxidation to metabolite M2, consistent with microsomal data (Figure 5). In human hepatocytes, however, metabolism of **12c** to both the oxidative metabolite M2 and the direct conjugation with glucuronic acid, designated M1, was equally prevalent. Disposition and metabolism of compound **12c** were

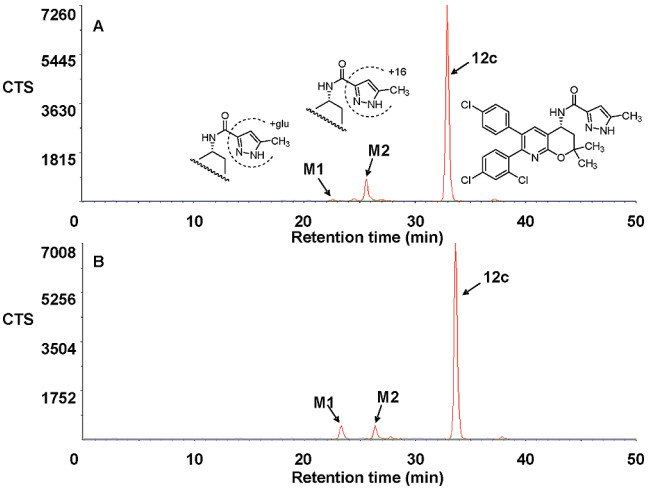

Figure 5. Representative radioprofiles of [^{3}H]**12c** following incubation (1 μM) with cryohepatocytes (3 million cells/mL) from (A) rat and (B) human.

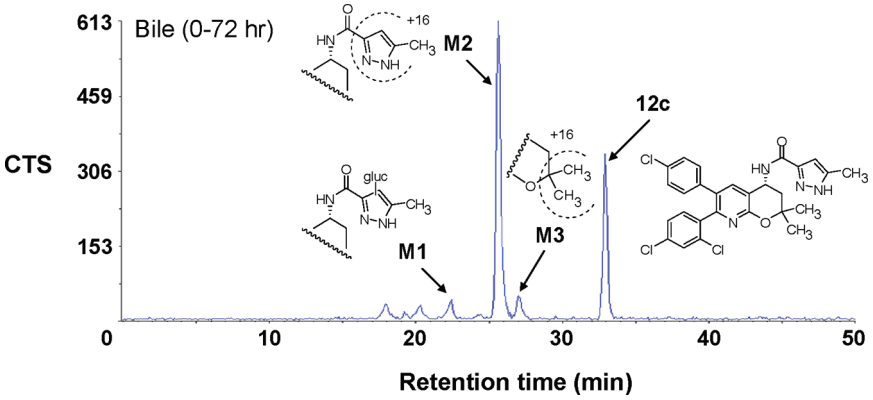

Figure 6. Metabolism profile of [^{3}H]**12c** in rat. Compound was formulated in Imwitor 742/Tween-80 (1:1) and dosed to bile duct cannulated rats po at 2 mg/kg. Bile was collected over a period of 72 h.

also evaluated in bile-duct-cannulated rats (Figure 6). Following oral dosing, the percentages of **12c** related radioactivity recovered over 72 h in feces, bile, and urine were 48%, 28%, and <1%, respectively, indicating that renal clearance was insignificant for this compound in the rat. The major radioactive component detected in bile was the intact parent (~30% of the absorbed dose), the parent glucuronide (M1, ~4%), and the oxidative metabolites M2 and M3. The major radioactive component in feces was the unabsorbed parent compound plus small amount of M2. Following the oral dosing, the major radioactive compound in rat plasma and the brain was the parent compound. The low levels of direct glucuronidation of parent observed in vivo in rats were consistent with data obtained in vitro in rat hepatocytes. The consistent metabolism profiles observed in vitro in hepatocytes as well as in vivo in rats suggested the potential for mixed metabolism in humans, where oxidative and direct glucuronidation pathways were comparable following incubation with human hepatocytes. The excretion of intact parent, likely due to Pgp-mediated efflux (see below), in rodents provided some additional support that clearance in man would not rely entirely on CYP mediated metabolism.

Susceptibility of compound **12c** to P-glycoprotein (P-gp) efflux transporter was evaluated in vivo by comparing levels of compound **12c** in the brain of wild type mouse (Mdr1a+/+) and P-gp deficient CF-1 mouse (Mdr1a−/−). After intravenous administration of **12c** at a dose of 1 mg/kg, the levels of parent (4 h postdose) were determined to be 410 nM in plasma and 270 nM in brain in wild type and to be 300 nM in plasma and 1400 nM in brain in P-gp deficient mouse. These data (brain to plasma ratio of 0.66 in wild type vs 4.66 in P-gp deficient CF-1 mouse) suggested that compound **12c** is a P-gp substrate.

The pharmacokinetic properties of compound **12c** were examined in three preclinical species (Table 3). Compound **12c** showed low systemic plasma clearance (1.1−4.5 (mL/min)/kg) across species and good elimination half-life in rat and monkey and long half-life in dog. Good oral bioavailability was observed in all species, with monkey the lowest at 46%.

Finally, compound **12c** was a moderate inhibitor of CYP3A4, CYP2C8, CYP2C9, and CYP2D6 with IC_{50} values of 3.3, 11, 18, and 6.0 μM, respectively, and was an activator of human pregnane X receptor (PXR) with an EC_{50} of ~5 μM and 55% activation response (at 5 μM) relative to rifampicin. Because of the structural resemblance to **2**, compound **12c** was evaluated in conscious mice for abnormal activity on CNS function at a single dose of 100 mg/kg. CNS assessments were conducted at 0.5, 1, 2, 5, and 24 h after dosing, and body temperature was measured at 2 h after dosing. Compound **12c** had no effect on CNS functions including gross behavior, neural reflexes, spontaneous activity, and thermoregulation during the 24 h period after dosing. Since **12c** has a hERG IC_{50} of 1 μM, its potential cardiovascular effect was examined by intravenously infusing **12c** evenly over 30 min with rising cumulative doses of 1, 3, and 10 mg/kg in anesthetized dogs. In comparison to vehicle-treated dogs, compound **12c** caused a modest reduction (~20%) in mean arterial pressure only at the highest dose. No changes in heart rat, electrocardiographic PR, ORS, and QTc cardiac intervals were observed in **12c**-treated dogs over this dose range. The peak plasma concentrations reached 1.63 ± 0.19, 3.26 ± 0.30, and 6.96 ± 0.33 μM during the administration of doses of 1, 3, and 10 mg/kg, respectively. Since **12c** was highly bound to plasma proteins (>99%) of rat, dog, monkey, and human at a concentration of 0.2 μM and only required low plasma concentration (<200 nM) to drive pharmacodynamic efficacy, compound **12c** should have a sufficient safety margin in a clinical study.

Table 3. Pharmacokinetics of Compound **12c** after Intravenous and Oral Administration in Rat, Dog, and Monkey[a]

	species		
pharmacokinetic parameter	rat	dog	monkey
Cl_p ((mL/min)/kg)	4.5	1.1	2.3
Vd_{ss} (L/kg)	3.0	5.7	2.4
$t_{1/2}$ (h)	8.5	60	15
C_{max} (μM)	1.03	0.15	0.09
F (%)	91	65	46
oral AUCN (μM·h·kg/mg)	11	18	6.1

[a] Pharmacokinetics were determined at doses of 1 mg/kg iv and 2 mg/kg po in male Sprague−Dawley rats and 0.2 mg/kg iv and 0.4 mg/kg po in male beagle dogs and rhesus monkeys. Intravenous pharmacokinetics were determined using a solution formulation in EtOH/PEG400/water (20:50:30, v/v/v) for rats and EtOH/PEG400/water (20:40:40 v/v/v) for dogs and monkeys. Oral pharmacokinetics were determined using a solution formulation in Imwitor742/Tween-80 (1:1 w/w) for rats, dogs, and monkeys.

In conclusion, a series of pyranopyridines containing functional groups suitable for glucuronidation of the parent compound were designed and synthesized as potent and selective CB1R inverse agonists. Several functional groups, such as trifluoroacetamide and substituted pyrazole groups, were identified to form glucuronide conjugates of the parent. Many of these compounds showed good pharmacodynamic efficacy to reduce overnight body weight and food intake in

DIO rats similar to lead compound **3**. Despite being a substrate of P-gp, compound **12c**, as a potent and selective CB1R inverse agonist, emerged as one of the most efficacious compounds in this series with attenuated off-target hERG activity. Compound **12c** demonstrated CB1R-related pharmacological efficacy similar to that of **1**, good pharmacokinetic profiles in preclinical species, acceptable safety margins, and a potentially balanced metabolism profile in man, allowing for further clinical evaluation as an antiobesity agent with lower potential of CYP3A4 mediated drug−drug interactions. Unfortunately, the development of several CB1 antagonists/inverse agonists, such as rimonabant (Sanofi-Aventis) and taranabant (**1**, Merck), was discontinued on the basis of concerns about adverse psychiatric effects, i.e., increased anxiety and depression or suicidal intentions.[20] Pfizer soon decided to discontinue the phase III development program for its investigational CB1 antagonist, i.e., CP-945,598, citing changing regulatory perspectives on the risk/benefit profile of the CB1 class.[21] In addition, the contradictory study results of rimonabant in psychiatric behavior animal models make it difficult to guide the selection of a preclinical candidate for development on the anticipation of improved psychiatric profile based on preclinical animal models.[22] Under such circumstances, clinical evaluation of **12c** as an antiobesity agent was no longer in progress. Nevertheless, the discovery of **12c** demonstrated the successful optimization of the metabolism profile of a CB1R inverse agonist without impacting its pharmacological properties.

Experimental Section

General. Unless noted otherwise, all materials were purchased from commercial sources and used without further purification. Reactions sensitive to moisture or air were performed under nitrogen or argon using anhydrous solvents and reagents. The progress of reactions was determined by either analytical thin layer chromatography (TLC), performed with E. Merck precoated TLC plates, silica gel 60F-254, and layer thickness of 0.25 mm, or liquid chromatography−mass spectrometry (LC−MS). Mass analysis was performed on a Waters Micromass ZQ with electrospray ionization in positive ion detection mode. High performance liquid chromatography (HPLC) was conducted on an Agilent 1100 series HPLC (LC-1), on Waters C18 XTerra 3.5 μm, 3.0 × 50 mm column with gradient 10:90 to 98:2 v/v CH_3CN/H_2O + v 0.05% TFA over 3.75 min then held at 98:2 v/v CH_3CN/H_2O + v 0.05% TFA for 1.75 min, with flow rate of 1.0 mL/min, UV wavelength of 254 nm, or (LC-2) on Waters C18 XTerra 3.5 μm, 2.1 mm × 20 mm column with gradient 10:90 to 98:2 v/v CH_3CN/H_2O + v 0.05% TFA over 3.25 min, then held at 98:2 v/v CH_3CN/H_2O + v 0.05% TFA for 0.75 min, with flow rate of 1.5 mL/min, UV wavelength 254 nm. Flash chromatography was performed using a Biotage flash chromatography apparatus (Dyax Corp.) on silica gel (32−63 mM, 60 Å pore size) in prepacked cartridges of the size noted. ^{1}H NMR spectra were acquired at 500 MHz spectrometers in $CDCl_3$ solutions unless otherwise noted. Chemical shifts were reported in parts per million (ppm). Tetramethylsilane (TMS) was used as internal reference in CD_3Cl solutions, and residual $\underline{CH_3}OH$ peak or TMS was used as internal reference in $\underline{CD_3}OD$ solutions. Coupling constants (J) were reported in hertz (Hz). Chiral analytical chromatography was performed on a Chiralpak AS, Chiralpak AD, Chiralcel OD, or Chiralcel OJ column (4.6 mm × 250 mm) (Daicel Chemical Industries, Ltd.) with noted percentage of either ethanol in hexane (%Et/Hex) or isopropanol in heptane (%IPA/Hep) as isocratic solvent systems. Chiral preparative chromatography was conducted on a Chiralpak AS, Chiralpak AD, Chiralcel OD, or Chiralcel OJ column (20 mm × 250 mm) (Daicel Chemical Industries, Ltd.) with the desired isocratic solvent systems identified on chiral analytical chromatography. The purity of all final compounds was determined by LC−MS to be ≥95%. Preparation of compound **12c** represents a typical procedure used for the synthesis of chiral compounds described therein.

6-(4-Chlorophenyl)-7-(2,4-dichlorophenyl)-2,2-dimethyl-2,3-dihydro-4*H*-pyrano[2,3-*b*]pyridin-4-one (5). To a solution of 6-(2,4-dichlorophenyl)-5-(4-chlorophenyl)-2-oxo-1,2-dihydropyridine-3-carbonitrile (**4**)[9] (15.7 g, 41.7 mmol) in THF (100 mL) was added 2-methyl-1-propenylmagnesium bromide (0.5 M in THF, 250 mL, 125 mmol). After being stirred at 50 °C overnight, the mixture was cooled and the reaction was quenched with 20 mL of H_2O. To the resulting mixture was added 100 mL of 2 N HCl, and the reaction mixture was stirred at room temperature for 20 min. The reaction mixture was poured into Et_2O (100 mL). The organic layer was separated and washed with H_2O (100 mL), saturated aqueous $NaHCO_3$ (2 × 100 mL), and brine. They organic layer was separated, dried over $MgSO_4$, and concentrated. The residue was purified by flash chromatography on a silica gel gradient, eluting with 0−25% EtOAc in hexane to afford the title compound (14.1 g, 78%): ^{1}H NMR δ 1.60 (s, 6H), 2.86 (s, 2H), 7.03−7.30 (m, 7H), 8.25 (s, 1H).

(4*S*)-6-(4-Chlorophenyl)-7-(2,4-dichlorophenyl)-2,2-dimethyl-3,4-dihydro-2*H*-pyrano[2,3-*b*]pyridin-4-ol (9). A mixture of compound **5** (14.1 g, 32.5 mmol) and [Ru(II)(η^6-arene)]-(*S*,*S*)-TsDPEN[11] (998 mg, 1.62 mmol) in IPA (20 mL) in CH_2Cl_2 (10 mL) was stirred at room temperature. After 16 h, the reaction mixture was concentrated to give the product, which was taken to the next step without further purification (9.8 g, 69.4%). ^{1}H NMR δ 1.43 (s, 3H), 1.56 (s, 3H), 1.96 (dd, J = 9.7, 13.4, 1H), 2.06 (d, J = 7.3, 1H), 2.28 (dd, J = 6.2, 13.5, 1H), 5.00 (m, 1H), 7.03 (d, J = 8.5, 2H), 7.18−7.26 (m, 5H), 7.90 (s, 1H).

(4*R*)-4-Azido-6-(4-chlorophenyl)-7-(2,4-dichlorophenyl)-2,2-dimethyl-3,4-dihydro-2*H*-pyrano[2,3-*b*]pyridine (10). To a mixture of **9** (9.8 g, 22.5 mmol), $Zn(N_3)_2$/bis-pyridine complex[13] (13.9 g, 45.1 mmol), triphenylphosphine (11.8 g, 45.1 mmol), and imidazole (6.1 g, 90 mmol) in 100 mL of CH_2Cl_2 was added diisopropyl azodicarboxylate (8.8 mL, 45.1 mmol) dropwise at room temperature. The mixture was allowed to stir at room temperature for 16 h. The supernatant was separated and washed with diluted HCl (1.0 N, 3 × 50 mL), saturated aqueous $NaHCO_3$ (3 × 50 mL), and brine (50 mL). The organic layer was separated, dried over $MgSO_4$, and concentrated. Chromatography on Biotage 40+M cartridges using 3:17 v/v EtOAc/hexanes as the eluant afforded the product (9.5 g, 92%): ^{1}H NMR δ 1.47 (s, 3H), 1.59 (s, 3H), 2.11 (dd, J = 9.6, 13.5, 1H), 2.32 (dd, J = 6.1, 13.6, 1H), 4.75 (dd, J = 6.0, 9.6, 1H), 7.04 (d, J = 8.5, 2H), 7.19−7.28 (m, 5H), 7.78 (s, 1H).

(4*R*)-6-(4-Chlorophenyl)-7-(2,4-dichlorophenyl)-2,2-dimethyl-3,4-dihydro-2*H*-pyrano[2,3-*b*]pyridin-4-amine (11). To a solution of **10** (9.5 g, 20.7 mmol) in 50 mL of THF was added 2.5 mL of H_2O and 31.0 mL of trimethylphosphine in THF (1.0 M, 31.0 mmol). After the mixture was stirred at room temperature for 3 h, the solvent was evaporated. Chromatography on a Biotage 40+M cartridge using 1:19 v/v CH_3OH/CH_2Cl_2 as the eluant gave the product (7.2 g, 80%): ^{1}H NMR δ 1.42 (s, 3H), 1.54 (s, 3H), 1.78 (t, J = 12.5, 1H), 2.18 (dd, J = 5.9, 13.4, 1H), 4.16 (dd, J = 6.0, 11.7, 1H), 7.04 (d, J = 8.5, 2H), 7.17−7.26 (m, 5H), 7.93 (s, 1H).

***N*-[(4*R*)-6-(4-Chlorophenyl)-7-(2,4-dichlorophenyl)-2,2-dimethyl-3,4-dihydro-2*H*-pyrano[2,3-*b*]pyridin-4-yl]-5-methyl-1*H*-pyrazole-3-carboxamide (12c).** A mixture of **11** (300 mg, 0.69 mmol), 5-methylpyrazole-3-carboxylic acid (105 mg, 0.83 mmol), PyBOP (540 mg, 1.04 mmol), and Et_3N (0.19 mL, 1.38 mmol) in 20 mL of CH_2Cl_2 was stirred at room temperature. After 16 h, the reaction mixture was diluted with Et_2O (50 mL) and washed with saturated aqueous $NaHCO_3$ (3 × 50 mL) and brine (3 × 50 mL). The organic layer was separated, dried over $MgSO_4$, and concentrated. Chromatography on a Biotage 40+S cartridge using 1:1 v/v

EtOAc/hexanes as the eluant afforded the desired product (344 mg, 92%): ^{1}H NMR δ 1.44 (s, 3H), 1.51 (s, 3H), 1.94 (t, J = 12.5, 1H), 2.26−2.30 (m, 4H), 5.62 (m, 1H), 6.58 (s, 1H), 6.96 (d, J = 8.5, 2H), 7.12−7.29 (m, 5H), 7.69 (s, 1H). The product purity was determined by LC−MS to be greater than 98%. Compound formula $C_{27}H_{23}Cl_3N_4O_2$, M_r = 541.840, orthorhombic, $P2_12_12_1$, a = 11.1695(8) Å, b = 11.2252(8) Å, c = 20.0044(14) Å, V = 2508.1(3) Å^3, Z = 4, D_x = 1.435 g cm^{-3}, monochromatized radiation λ(Mo) = 0.710 73 Å, μ = 0.40 mm^{-1}, F(000) = 1120, T = 100 K. Data were collected on a Bruker CCD diffractometer to a θ limit of 28.64° which yielded 34 470 reflections. There are 6426 unique reflections with 5500 observed at the 2σ level. The structure was solved by direct methods (SHELXS-97; Sheldrick, G. M. *Acta Crystallogr*. **1990**, *A46*, 467−473) and refined using full-matrix least-squares on F^2 (SHELXL-97; Sheldrick, G. M. *SHELXL-97. Program for the Refinement of Crystal Structures*; University of Göttingen: Göttingen, Germany). The final model was refined using 322 parameters and all 6426 data. All non-hydrogen atoms were refined with isotropic thermal displacements. The final agreement statistics are as follows: R = 0.043 (based on 5500 reflections with I > 2σ(I)), wR = 0.090, S = 1.17 with $(\Delta/\sigma)_{max}$ = 0.01. The maximum peak height in a final difference Fourier map is 0.293 e Å^{-3}, and this peak is without chemical significance. CCDC contains the supplementary crystallographic data for this paper (CCDC deposition number 760723). These data can be obtained free of charge from The Cambridge Crystallographic Data Centre via www.ccdc.cam.ac.uk/data_request/cif.

Acknowledgment. The authors thank Dr. William K. Hagmann for useful discussions about the manuscript, Dr. Vincent J. Colandrea for useful discussion regarding the Noyori chemistry, and Dr. Hugo Vargas and Patricia Bunting (Department of Safety Assessment, Merck Research Laboratories, West Point, PA 19486) for CV dog and CNS mice studies.

Supporting Information Available: ^{1}H NMR, LC−MS, and chiral analytical HPLC data for compounds **3**, **13**−**16**, **8a**−**8h**, **12a**, **12b**, **12d**−**n**; crystallographic data in CIF format. This material is available free of charge via the Internet at http://pubs.acs.org.

References

(1) World Health Organization. Obesity Fact Sheet. http://www.who.int/mediacentre/factsheets/fs311/en/index.html (accessed January 6, **2010**).

(2) Finkelstein, E. A.; Trogdon, J. G.; Cohen, J. W.; Dietz, W. Annual medical spending attributable to obesity: payer- and service-specific estimates. *Health Affairs* **2009**, *28*, w822–w831.

(3) Crowley, V. E. F. Overview of human obesity and central mechanisms regulating energy homeostasis. *Ann. Clin. Biochem.* **2008**, *45*, 245–255.

(4) (a) Woods, S. C.; D'Alessio, D. A. Central control of body weight and appetite. *J. Clin. Endocrinol. Metab.* **2008**, *93*, S37–S50. (b) Kunos, G.; Osei-Hyiaman, D.; Liu, J.; Godlewski, G.; Batkai, S. Endocannabinoids and the control of energy homeostasis. *J. Biol. Chem.* **2008**, *283*, 33021–33025.

(5) (a) Akbas, F.; Gasteyger, C.; Sjodin, A.; Astrup, A.; Larsen, T. M. A critical review of the cannabinoid receptor as a drug target for obesity management. *Obes. Rev.* **2009**, *10*, 58–67. (b) Janero, D. R.; Makriyannis, A. Cannabinoid receptor antagonists: pharmacological opportunities, clinical experience, and translational prognosis. *Expert Opin. Emerging Drugs* **2009**, *14*, 43–65.

(6) (a) Plummer, C. W.; Finke, P. E.; Mills, S. G.; Wang, J.; Tong, X.; Doss, G. A.; Fong, T. M.; Lao, J. Z.; Schaeffer, M.-T.; Chen, J.; Shen, C.-P.; Stribling, D. S.; Shearman, L. P.; Strack, A. M.; Van der Ploeg, L. H. T. Synthesis and activity of 4,5-diarylimidazoles as human CB1 receptor inverse agonist. *Bioorg. Med. Chem. Lett.* **2005**, *15*, 1441–1446. (b) Debenham, J. S.; Madsen-Duggan, C. B.; Walsh, T. F.; Wang, J.; Tong, X.; Doss, G. A.; Lao, J.; Fong, T. M.; Schaeffer, M.-T.; Xiao, J. C.; Huang, C. R.-R. C.; Shen, C.-P.; Feng, Y.; Marsh, D. J.; Stribling, D. S.; Shearman, L. P.; Strack, A. M.; MacIntyre, D. E.; Van der Ploeg, L. H. T.; Goulet, M. T. Synthesis of functionalized 1,8-naphthyridinones and their evaluation as novel, orally active CB1 receptor inverse agonists. *Bioorg. Med. Chem. Lett.* **2006**, *16*, 681–685. (c) Lin, L. S.; Lanza, T. J.; Jewell, J. P.; Liu, P.; Shah, S. K.; Qi, H.; Tong, X.; Wang, J.; Xu, S. S.; Fong, T. M.; Shen, C.-P.; Lao, J.; Xiao, J. C.; Shearman, L. P.; Stribling, D. S.; Rosko, K.; Strack, A.; Marsh, D. J.; Feng, Y.; Kumar, S.; Samuel, K.; Yin, W.; Van der Ploeg, L. H. T.; Goulet, M. T.; Hagmann, W. K. Discovery of N-[(1S,2S)-3-(4-chlorophenyl)-2-(3-cyanophenyl)-1-methylpropyl]-2-methyl-2-{[5-(trifluoromethyl)pyridine-2-yl]oxy}propanamide (MK-0364), a novel, acyclic cannabinoid-1 receptor inverse agonist for the treatment of obesity. *J. Med. Chem.* **2006**, *49*, 7584–7587. (d) Armstrong, H. E.; Galka, A.; Lin, L. S.; Lanza, T. J.; Jewell, J. P.; Shah, S. K.; Guthikonda, R.; Truong, Q.; Chang, L. L.; Quaker, G.; Colandrea, V. J.; Tong, X.; Wang, J.; Xu, S. S.; Fong, T. M.; Shen, C.-P.; Lao, J.; Chen, J.; Shearman, L. P.; Stribling, D. S.; Rosko, K.; Strack, A.; Ha, S.; Van der Ploeg, L. H. T.; Goulet, M. T.; Hagmann, W. K. Substituted acyclic sulfonamides as human cannabinoid-1 receptor inverse agonists. *Bioorg. Med. Chem. Lett.* **2007**, *17*, 2184–2187. (e) Liu, P.; Lin, L. S.; Hamill, T. G.; Jewell, J. P.; Lanza, T. J.; Gibson, R. E.; Krause, S. M.; Ryan, C.; Eng, W.; Sanabria, S.; Tong, X.; Wang, J.; Levorse, D. A.; Owens, K. A.; Fong, T. M.; Shen, C.-P.; Lao, J.; Kumar, S.; Yin, W.; Payak, J. F.; Springfield, S. A.; Hargreaves, R.; Burns, H. D.; Goulet, M. T.; Hagmann, W. K. Discovery of N-{(1S,2S)-2-(3-cyanophenyl)-3-[4-(2-[^{18}F]fluoroethoxy)phenyl]-1-methylpropyl}-2-methyl-2-[(5-methylpyridin-2-yl)oxy]propanamide, a cannabinoid-1 receptor positron emission tomography tracer suitable for clinical use. *J. Med. Chem.* **2007**, *50*, 3427–3430. (f) Debenham, J. S.; Madsen-Duggan, C. B.; Wang, J.; Tong, X.; Lao, J.; Fong, T. M.; Schaeffer, M.-T.; Xiao, C. J.; Huang, C. C. R.-R.; Shen, C.-P.; Stribling, D. S.; Shearman, L. P.; Strack, A. M.; MacIntyre, D. E.; Hale, J. J.; Walsh, T. F. Pyridopyrimidine based cannabinoid-1 receptor inverse agonists: synthesis and biological evaluation. *Bioorg. Med. Chem. Lett.* **2009**, *19*, 2591–2594. (g) Vachal, P.; Fletcher, J. M.; Fong, T. M.; Huang, C. C. R.-R.; Lao, J.; Xiao, C. J.; Shen, C.-P.; Strack, A.; Shearman, L.; Stribling, S.; Chen, R. Z.; Frassetto, A.; Tong, X.; Wang, J.; Ball, R,. G.; Tsou, N. N.; Hickey, G. J.; Thompson, D. F.; Faidley, T. D.; Nicolich, S.; Achanfuo-Yeboah, J.; Hora, D. F.; Hale, J. J.; Hagmann, W. K. 1-Sulfonyl-4-acylpiperazines as selective cannabinoid-1 receptor (CB1R) inverse agonists for the treatment of obesity. *J. Med. Chem.* **2009**, *52*, 2550–2558. (h) Du, W.; Jewell, J. P.; Lin, L. S.; Colandrea, V. J.; Xiao, J. C.; Lao, J.; Shen, C.-P.; Bateman, T. J.; Reddy, V. B. G.; Ha, S. N.; Shah, S. K.; Fong, T. M.; Hale, J. J.; Hagmann, W. K. Synthesis and evaluation of N-[(1S,2S)-3-(4-chlorophenyl)-2-(3-cyanophenyl)-1-methylpropyl]-2-methyl-2-aminopropanamide as human cannabinoid-1 receptor (CB1R) inverse agonists. *Bioorg. Med. Chem. Lett.* **2009**, *19*, 5195–5199.

(7) (a) Hagmann, W. K. The discovery of taranabant, a selective cannabinoid-1 receptor inverse agonist for the treatment of obesity. *Arch. Pharm.* (*Weinheim, Ger.*) **2008**, *341*, 405–411. (b) Gantz, I.; Erondu, N.; Suryawanshi, S.; Musser, B.; Nayee, J.; Johnson-Levonas, A. O.; Heymsfield, S.; Amatruda, J. A Two-Year Study To Assess the Efficacy, Safety, and Tolerability of Taranabant in Obese Patients: 52 Week Results. Presented at the 57th Annual Scientific Session, Peripheral Arterial Disease; Pharmacology/Hormones—Basic and Clinical 1021-220, American College of Cardiology, Chicago, IL, March 31 through April 1, **2008**.

(8) (a) Schwartz, J. I.; Dunbar, S.; Yuan, J.; Li, S.; Miller, D. L.; Rosko, K.; Johnson-Levonas, A. O.; Lasseter, K. C.; Wagner, J. A. Influence of taranabant, an orally active, highly selective, potent cannabinoid-1 receptor (CB1R) inverse agonist, on ethinyl estradiol and norelegestromin plasma pharmacokinetics. *J. Clin. Pharmacol.* **2009**, *49*, 72–79. (b) Addy, C.; Rothenberg, P.; Li, S.; Majumdan, A.; Agrawal, N.; Li, H.; Zhong, L.; Yuan, J.; Maes, A.; Dunbar, S.; Cote, J.; Rosko, K.; Van Dyck, K.; De Lepeleire, I.; de Hoon, J.; Van Hecken, A.; Depre, M.; Knops, A.; Gottensdiener, K.; Stoch, A.; Wagner, J. Multiple-dose pharmacokinetics, pharmacodynamics, and safety of taranabant, a novel selective cannabinoid-1 receptor inverse agonist, in healthy male volunteers. *J. Clin. Pharmacol.* **2008**, *48*, 734–744.

(9) (a) Debenham, J. S.; Madsen-Duggan, C. B.; Toupence, R. B.; Walsh, T. F.; Wang, J.; Tong, X.; Kumar, S.; Lao, J.; Fong, T. M.; Xiao, J. C.; Huang, C. R.-R. C.; Shen, C. P.; Feng, Y.; Marsh, D. J.; Stribling, D. S.; Shearman, L. P.; Strack, A. M.; Goulet, M. T. Furo[2,3-*b*]pyridine-based cannabinoid-1 receptor inverse agonists: synthesis and biological evaluation part 1. *Bioorg. Med. Chem. Lett.* **2010**, *20*, 1448–1452. (b) Madsen-Duggan, C. B.; Debenham, J. S.; Walsh, T. F.; Yan, L.; Huo, P.; Wang, J.; Tong, X. S.; Lao, Z. J.; Fong, T. M.; Xiao, J. C.; Huang, R. C.; Shen, C.; Stribling, D. S.; Shearman, L. P.; Strack, A. M.; Goulet, M. T.; Hale, J. J. Dihydro-pyrano[2,3-b]pyridines and tetrahydro-1,8-naphthyridines as CB1 receptor inverse agonists: synthesis, SAR and biological evaluation. *Bioorg. Med. Chem. Lett.*, manuscript accepted.

(10) Debenham, J. S.; Hale, J. J.; Huo, P.; Madsen-Duggan, C. B.; Walsh, T. F.; Yan, L. Substituted Pyrano[2,3-*b*]pyridine Derivatives as Cannabinoid-1 Receptor Modulators and Their Preparation, Pharmaceutical Compositions and Use in the Treatment of Diseases. WO 2008094473 A1 20080807, 2008.
(11) Haack, K.-J.; Hashiguchi, S.; Fujii, A.; Ikariya, T.; Noyori, R. The catalyst precursor, catalyst, and intermediate in the Ru^{II}-promoted asymmetric hydrogen transfer between alcohols and ketones. *Angew. Chem., Int. Ed. Engl.* **1997**, *36*, 285–288.
(12) For better separation on chiral HPLC, *S*-alcohol **9** and its *R*-enantiomer were converted to their corresponding benzoate esters. The enantiomeric enrichment was determined by chiral HPLC on ChiralCel OJ 250 mm × 4.6 mm i.d. and 10 μm silica gel column with isocratic 5% EtOH in hexane over 40 min, flow rate of 0.75 mL/min, wavelength of 254 nm.
(13) Viaud, M. C.; Rollin, P. Zinc azide mediated Mitsunobu substitution, an expedient method for the one-pot azidation of alcohols. *Synthesis* **1990**, 130–132.
(14) *R*-Amine **11** and its *S*-enantiomer were converted to their corresponding acetamides. The enantiomeric enrichment was determined by chiral HPLC on ChiralPak AS 250 mm × 4.6 mm i.d. and 10 μm silica gel column with isocratic 7% EtOH in hexane over 40 min, flow rate of 0.75 mL/min, and wavelength of 254 nm.
(15) (a) Rowland, M.; Matin, S. B. Kinetics of drug−drug interactions. *J. Pharmacokinet. Biopharm.* **1973**, *1*, 553–567. (b) Ito, K.; Hallifax, D.; Obach, R. S.; Houston, J. B. Impact of parallel pathways of drug elimination and multiple cytochrome P450 involvement on drug−drug interactions: CYP2D6 paradigm. *Drug Metab. Dispos.* **2005**, *33*, 837. (c) Shipkova, M.; Wieland, E. Glucuronidation in therapeutic drug monitoring. *Clin. Chim. Acta* **2005**, *358*, 2–23.
(16) For detailed procedures for in vitro pharmacology and in vivo food intake and body weight studies in mouse and DIO rats, reference to the following: Fong, T. M.; Guan, X.-M.; Marsh, D. J.; Shen, C.-P.; Stribling, D. S.; Rosko, K. M.; Lao, J.; Yu, H.; Feng, Y.; Xiao, J. C.; Van der Pleog, L. H. T.; Goulet, M. T.; Hagmann, W. K.; Lin, L. S.; Lanza, T. J.; Jewell, J. P.; Liu, P.; Shah, S. K.; Qi, H.; Tong, X.; Wang, J.; Xu, S. S.; Francis, B.; Strack, A. M.; MacIntyre, D. E.; Shearman, L. P. Antiobesity efficacy of a novel cannabinoid-1 receptor inverse agonist, *N*-[(1*S*,2*S*)-3-(4-chlorophenyl)-2-(3-cyanophenyl)-1-methylpropyl]-2-methyl-2-{[5-(trifluoromethyl)pyridine-2-yl]oxy}propanamide (MK-0364), in rodents. *J. Pharmacol. Exp. Ther.* **2007**, *321*, 1013–1022.
(17) Wang, J.; Della Penna, K.; Wang, H.; Karczewski, J.; Connolly, T. M.; Koblan, K. S.; Bennett, P. B.; Salata, J. J. Functional and pharmacological properties of canine ERG potassium channels. *Am. J. Physiol.: Heart Circ. Physiol.* **2003**, *284*, H256–H267.
(18) Metabolism studies were analyzed on a Shimadzu HPLC coupled to a Thermo Finnagan LTQ mass spectrometer, equipped with a Packard flow scintillation analyzer.
(19) (a) Chen, R. Z.; Frassetto, A.; Lao, J. Z.; Huang, R.-R. C.; Xiao, J. C.; Clements, M. J.; Walsh, T. F.; Hale, J. J.; Wang, J.; Tong, X.; Fong, T. M. Pharmacological evaluation of LH-21, a newly discovered molecule that binds to cannabinoid CB_1 receptor. *Eur. J. Pharmacol.* **2008**, *584*, 338–342. (b) Zimmer, A.; Zimmer, A. M.; Hohmann, A. G.; Herkenham, M.; Bonner, T. I. Increased mortality, hypoactivity, and hypoalgesia in cannabinoid CB1 receptor knockout mice. *Proc. Natl. Acad. Sci. U.S.A.* **1999**, *96*, 5786–5790.
(20) Di Marzo, V.; Després, J.-P. CB1 antagonists for obesity—what lessons have we learned from rimonabant? *Nat. Rev. Endocrinol.* **2009**, *5*, 633–638.
(21) Griffith, D. A.; Hadcock, J. R.; Black, S. C.; Iredale, P. A.; Carpino, P. A.; DaSilva-Jardine, P.; Day, R.; DiBrino, J.; Dow, R. L.; Landis, M. S.; O'Connor, R. E.; Scott, D. O. Discovery of 1-[9-(4-chlorophenyl)-8-(2-chlorophenyl)-9*H*-purin-6-yl]-4-ethylamino-piperidine-4-carboxylic acid amide hydrochloride (CP-945,598), a novel, potent, and selective cannabinoid type 1 receptor antagonist. *J. Med. Chem.* **2009**, *52*, 234–237.
(22) (a) Griebel, G.; Stemmelin, J.; Scatton, B. Effects of the cannabinoid CB1 receptor antagonist rimonabant in models of emotional reactivity in rodents. *Biol. Psychiatry* **2005**, *57*, 261–267. (b) Wiley, J. L.; Martin, B. R. Cannabinoid pharmacological properties common to other centrally acting drugs. *Eur. J. Pharmacol.* **2003**, *471*, 185–193. (c) Navarro, M.; Hernández, E.; Muñoz, R. M.; del Arco, I.; Villanúa, M. A.; Carrera, M. R. A.; de Fonseca, F. R. Acute administration of the CB_1 cannabinoid receptor antagonist SR 141716A induces anxiety-like responses in the rat. *NeuroReport* **1997**, *8*, 491–496.